

Wave Generation with a Hydrofoil by More Efficient Free-Surface Boundary Condition

S. H. Kwag*

고효율 자유표면 경계조건에 의한 수중익 주위의 파도생성

곽 승 현

Key Words : Free Surface(자유표면), FDM(유한차분법), Navier-Stokes(나비에 스톡스), MAC (Marker and Cell), Submerged Wing(수중날개)

Abstract

For the calculation of the free-surface elevation, a new finite difference scheme is studied where the third derivative term for the wave elevation is artificially added in the Eulerian expression of the free-surface boundary condition. The paper presents a comparative analysis with simulations performed by the classical MAC method. More schematic computations are carried out by changing the submergence-depth and angle-of-attack. The present study shows that this new method is very efficient for the simulation of free-surface elevation around the trailing edge.

1. Introduction

The wave-body interaction and free surface treatment is related to the design of the high speed craft. Although the theory of such bodies running near the free-surface is not new, almost all the former investigations were concerned with the computation of the overall forces on the body namely lift and drag.

Recently some works have been directed to the solution of Navier-Stokes equations accounting for the presence of a free-surface. Works where free-surface problems were studied using finite difference methods include Mori^[1], Lungu^[2] and Hinatsu^[3]. Field discretization methods have some inherent limitations. With any workable numerical scheme, 'numerical viscosity' is also present. This introduces a

* 정회원, 한라공과대학교 조선공학과 부교수

numerical diffusion phenomenon in addition to the physical diffusion and gives incorrect solutions for large Reynolds numbers. It is still beyond modern computational capabilities to use grid sizes even being sufficiently small that numerical viscosity effects can be reduced to satisfactory levels at realistic Reynolds numbers. Based on the above considerations, some computations were carried out by Fujita^[4] in order to study the possibility of using a new computational method of the free-surface elevation. In this paper, the third-derivative term is applied for the 3-D case which seems to be an extension work of Fujita, Lungu and Mori^[5]. Further schematic computations and studies on the grid size are carried out in the present research.

2. Numerical Scheme

2.1 Governing Equations

The Navier-Stokes and continuity equations are used in the numerical simulation, which can be seen in the text of fluid dynamics.

2.2 Boundary Condition

At the upstream the flow starts from zero and is accelerated up to the predefined speed. Thus, each horizontal component of velocity has the constant value depending on the time step. The vertical component is equal to zero in each point of the upstream boundary and remains the same during the pressure computation. The pressure is the static one and remains the same, too. The bottom boundary is located far enough from the still water level. That means the wavy motion

influence is so gentle that the zero gradient extrapolation can be used for both components of velocity. The pressure is set constant at the static value. On the body surface, the no-slip condition and the Neumann conditions are used.

2.3 Free-Surface Treatment

The information on the location of the free-surface at each grid point and its slope and curvature is obtained by

$$\frac{\partial \zeta}{\partial t} + u \frac{\partial \zeta}{\partial x} + v \frac{\partial \zeta}{\partial y} - w = 0 \Big|_{z=\zeta} \quad (1)$$

The relations are of the first order of approximation for x , y and ζ . The use of (1) to determine the new location of the particle on the free-surface means to define the position locally, not taking into account the influence of the neighbouring particle movements which can accelerate the wave development. On the other hand, the use of an Euler-type expression of the kinematic free-surface boundary condition makes possible to employ a higher finite difference scheme. The following condition can be written as

$$\frac{\partial \zeta}{\partial t} \Big|_{k+1} + (u_i + \frac{\partial u}{\partial z} \Delta \zeta_i) \frac{\partial \zeta^{k+1}}{\partial x} - (w_i + \frac{\partial w}{\partial z} \Delta \zeta_i) = 0 \quad (2)$$

Expanding in Taylor series the function ζ at the $(k+1)$ and k -th time step, and then subtracting, we can get

$$\left. \frac{\partial \zeta}{\partial t} \right|_{k+1} = \frac{1}{2} (\zeta^{k-1} - 4\zeta^k + 3\zeta^{k+1}) \frac{1}{\Delta t} \quad (3)$$

Here we introduce the third derivative term which contributes the phase shift without damping. It can be obtained by the Taylor expansions.

$$\frac{\alpha c}{6\Delta x} (\zeta_{i-3} - 3\zeta_{i-2} + 3\zeta_{i-1} - \zeta_i); \quad (4)$$

where α is a constant. (4) is added to the TOUD(third order upwind difference), and the new formulation for the $\partial \zeta / \partial x$, which will be used in the free-surface definition, can be written :

$$\left. \frac{\partial \zeta^{k+1}}{\partial x} \right|_i = \frac{1}{6\Delta x} (-\zeta_{i-3}^{k+1} + 6\zeta_{i-2}^{k+1} - 15\zeta_{i-1}^{k+1} + 10\zeta_i^{k+1}) \quad (5)$$

Substituting (4) and (5) into (2), we can get :

$$\begin{aligned} & \frac{1}{2\Delta t} (\zeta_i^{k-1} - 4\zeta_i^k + 3\zeta_i^{k+1}) + (u_i + \frac{\partial u}{\partial z} \Delta \zeta_i) \cdot \\ & \frac{1}{6\Delta x} (-\zeta_{i-3}^k + 6\zeta_{i-2}^k - 15\zeta_{i-1}^k + 10\zeta_i^k - \\ & \quad \underbrace{\hspace{10em}}_{Fk} \\ & \quad \underbrace{\Delta \zeta_{i-3} + 6\Delta \zeta_{i-2} - 15\Delta \zeta_{i-1} + 10\Delta \zeta_i}_{\Delta F}) - \\ & (w_i + \frac{\partial w}{\partial z} \Delta \zeta_i) = 0 \end{aligned} \quad (6)$$

By manipulating above relations,

$$\begin{aligned} & \Delta \zeta_{i-1} - (\zeta_i - \zeta_{i-1})^k = \\ & \zeta_{i-1}^{k+1} - \zeta_{i-1}^k - \zeta_i^k + \zeta_{i-1}^k = \zeta_{i-1}^{k+1} - \zeta_i^k \end{aligned} \quad (7)$$

$$\Delta \zeta_i = \zeta_i^{k+1} - \zeta_i^k \quad (8)$$

Therefore, we finally can use the following equations.

$$\begin{aligned} \zeta_i^{k+1} = \zeta_i^k + & \left[\frac{u_i}{\Delta x} (\zeta_{i-1}^{k+1} - \zeta_i^k) + w_i + \right. \\ & \left. \frac{1}{2\Delta t} (\zeta_i^k - \zeta_i^{k-1}) \right] / F' \end{aligned} \quad (9)$$

where,

$$\begin{aligned} F' = \frac{3}{2\Delta t} + \frac{u_i}{\Delta x} + \frac{\partial u}{\partial z} (\zeta_i^k - \zeta_{i-1}^k) \\ \frac{1}{\Delta x} - \frac{\partial w}{\partial z} \end{aligned} \quad (10)$$

3. Results and Discussion

3.1 Computational Condition

The present work consists the numerical calculation of three dimensional hydrofoil. The ratio of span/chord is 3.0 with the shape of NACA 0012 wing section in the spanwise direction at 10° and 20°, angle of attack. The submergence depth is 0.4 and 0.8 respectively. The computing domain is 3.5 times the chord length in the streamwise direction. The computational conditions are tabulated in Table 1. The grid is made as H-H topology to treat the free-surface movement more conveniently, but relatively a large number of iterations are requested near the lines around the leading edge. Fig.1 shows the coordinate system for the computation ; x, y and z represent coordinates in a Cartesian system, x in the

uniform flow direction, y in the lateral and z normal to the x - y plane. Fig.2 shows the mesh system and computing domain. The number of grid used here is extremely insufficient to simulate the flows in all interesting regions, but some places are relatively clustered, for example, near the body surface, around tip and trailing edges, and beneath the free-surface.

Table 1 Computational conditions

	case A	case B	case C
d/L	0.4	0.8	0.8
α	20°	20°	10°

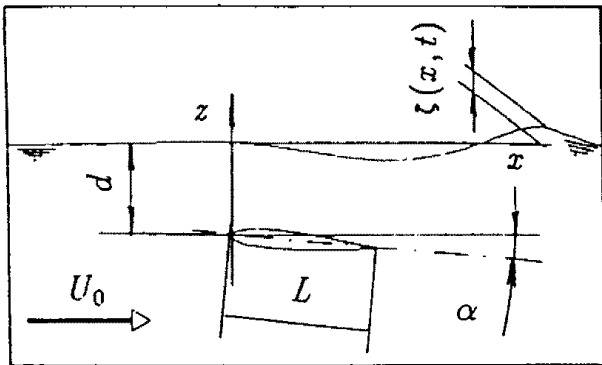


Fig. 1 Coordinates system

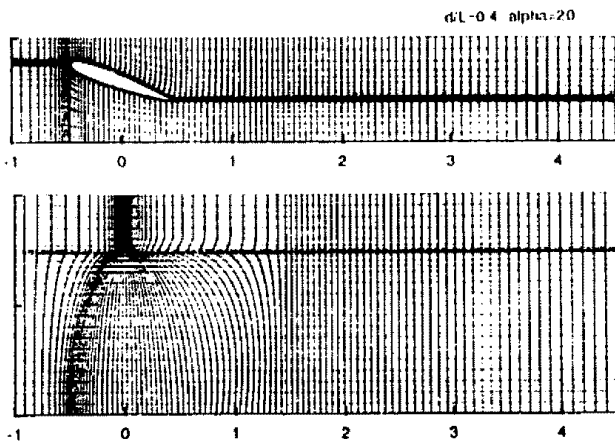


Fig. 2 Mesh system and computing domain

3.2 Discussions

The free-surface wave profiles are shown in Fig.3 which presents a comparison between the old(MAC) method and the new numerical scheme for the free-surface boundary condition at $T=3.0$ where T is the non-dimensionalized time. The zero-extrapolation is used at the downstream for both of them. As can be seen, the free-surface wave has reasonably developed by using the new finite difference scheme of the Euler-type formulation. It is a result of the third derivative introduced in the simulation. The new method is on the whole successful, but it is quite conspicuous especially in the shallow submergence case. The effect of angle-of-attack and submergence depth can be seen in case B and case C. This numerical result demonstrates that the new finite method does not cast a doubt on its validity. Fig.4 shows the pressure contours computed by the MAC method and the new method. The pressure difference can be seen near the free-surface for both cases. However, there is hardly seen any difference near the wing surface. Fig.5 shows the pressure contours on the wing surface. The above two figures belong to the suction side and below two to the pressure side. In case of the new method, the pressure gradient is comparatively modest. The new method gives rise to some wiggles in the contour lines. This may be due to the numerical instability. Fig.6 shows the velocity vectors in the whole domain. Here, (a) and (b) correspond to the midspan section for case A. The velocity defect can be seen clearly for both cases, but the fully generated free-surface of (b) makes some differences in the point of

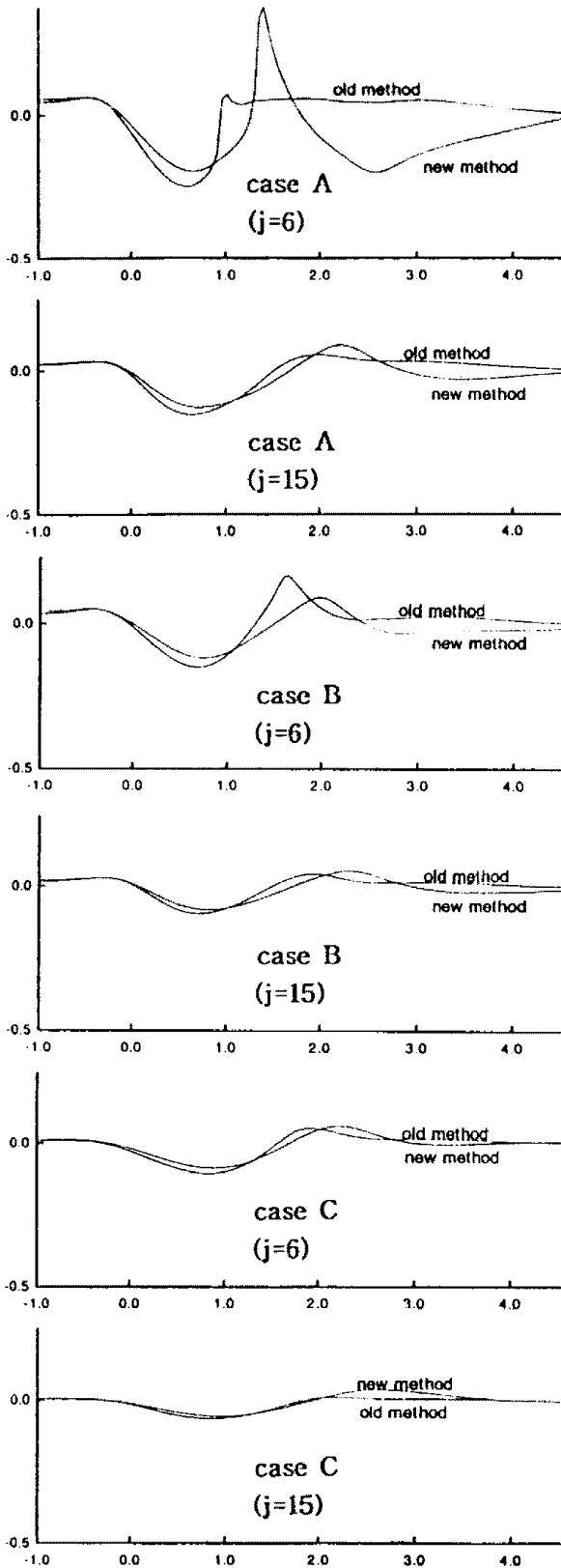


Fig. 3 Free-surface profiles computed by using the old(MAC) method and the new finite difference scheme

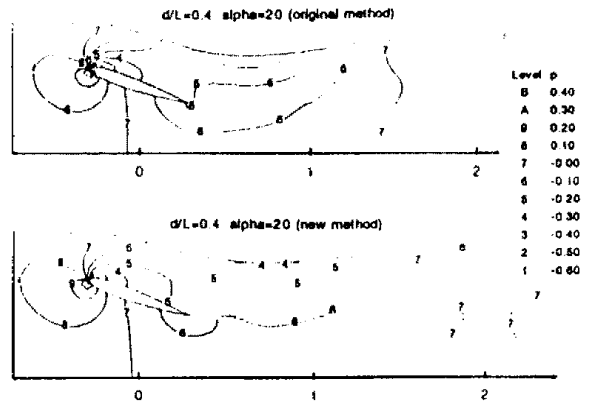


Fig. 4 Pressure contours computed by the original(MAC) method and the new (finite difference) method

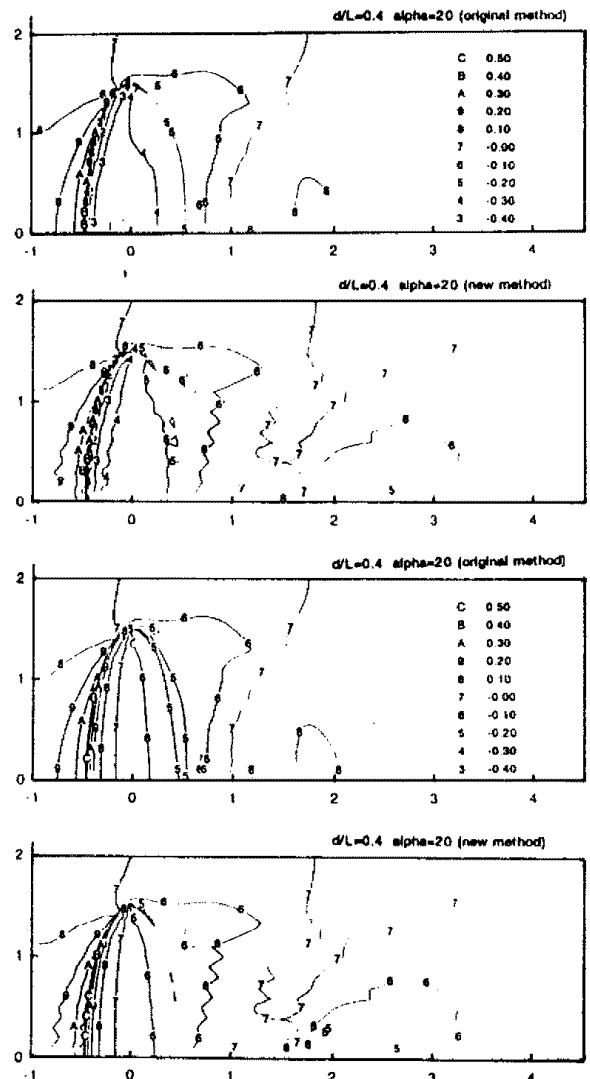


Fig. 5 Pressure contours on 3-D wing surface (above two belong to suction side, below two to pressure side)

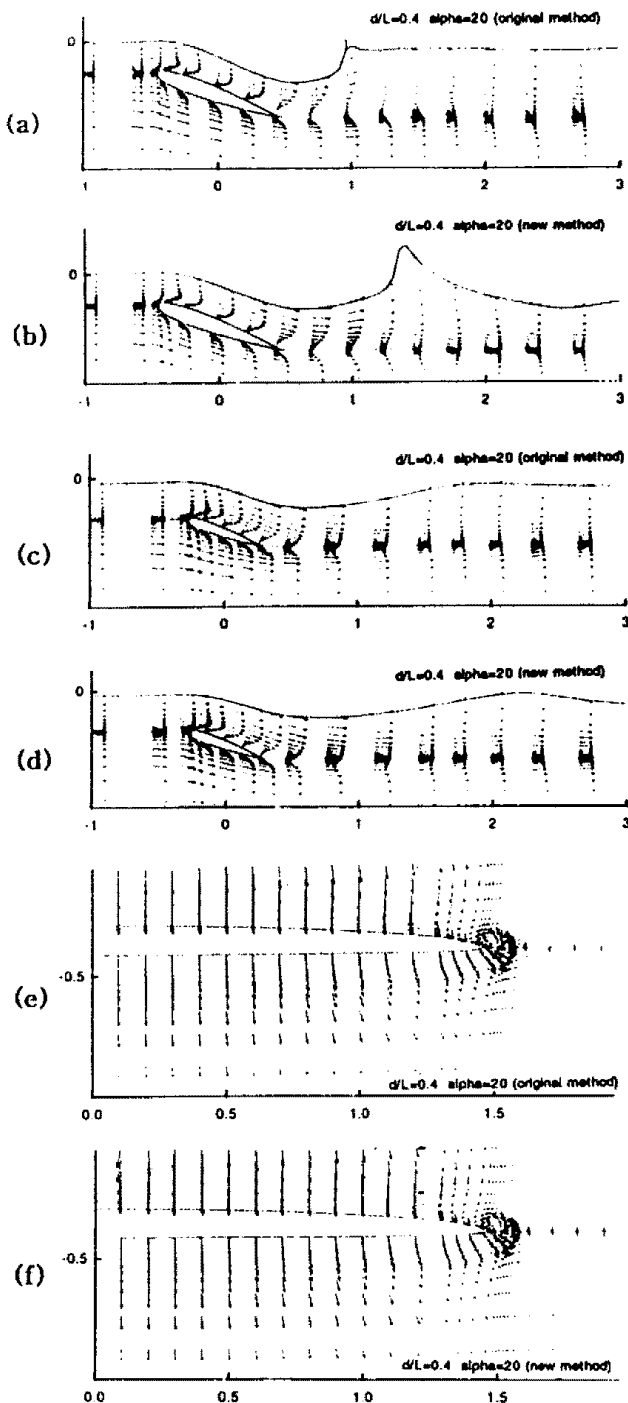


Fig. 6 Velocity vectors for case A

- (a), (b) : x-z plane ($j=6$)
 (c), (d) : x-z plane ($j=15$)
 (e), (f) : y-z plane ($j=27$)

vector direction and magnitude. (c) and (d) correspond to the near-tip section for case A,

where we can't see any significant discrepancies. (e) and (f) show the velocity vector in y-z plane. The two methods show similar phenomena, i.e., vortical motion around the tip.

4. Conclusion

For the validation of the numerical scheme, the flows around the three dimensional submerged wing is investigated by carrying out some comparative computations. Findings are as follows :

- 1) The free-surface wave can be generated at the large angle of attack 20° which usually gives some numerical trouble of the divergence. It means that the N-S solver can treat free-surface viscous flows more efficiently with the new finite difference scheme.
- 2) The finite difference method with the third derivative gives the better results in the free-surface generation. The wave in the far downstream can be made even if the grid number is so limited.

요 약

항공공학 분야의 해양파 문제에서 비선형이 강한 자유수면 문제를 수치적으로 해석하였다. 자유수면 격자를 유한차분법의 이산화 과정을 통해 재연한 것으로 자유표면 경계조건에 3차 미분항을 추가시켜 수치실험을 수행하였다. MAC 방법에 새로운 수치기법을 도입하여 수면깊이 및 받음각에 따른 수치결과를 기존의 방법과 상호 비교하였다. 본 수치연구는, 점성유동장 계산에서 3차 풍상미분항이 자유표면파 생성에 효과가 크게 나타남을 보여 주었다.

References

- 1) Mori, K., "New treating of the free-surface and downstream boundary condition in numerical computations of free-surface flows", Proceeding of seventh International Workshop on Water Waves and Floating Bodies, 1992, pp. 205-208.
- 2) Lungu, A., Mori, K., "New finite difference method for efficient and accurate free-surface flow computation", Proceeding of The Sixth Conference on CFD, Tokyo, 1992, pp. 389-393.
- 3) Hinatsu, M., "Numerical simulation of unsteady viscous nonlinear waves using moving grid system fitted on a free surface", Jour. of the Kansai Soc. of Naval Arch. Japan, nr. 217, 1992, pp. 1-11
- 4) Fujita, K. "On more accurate and efficient methods for the free-surface flow computations by the finite difference method", Master Thesis, Hiroshima University, 1992, (in Japanese).
- 5) Lungu, A., Mori, K., "A study on numerical schemes for more accurate and efficient computations of free-surface flows by finite difference method", Journal of the Society of Naval Architects of Japan, vol.173, 1993, pp. 9-17.

Appendix

The govern equations are the Navier-Stokes and continuity equations.

$$u_t + uu_x + vu_y + wu_z = -p_x + \frac{1}{R_n} \nabla^2 u$$

$$v_t + uv_x + vv_y + wv_z = -p_y + \frac{1}{R_n} \nabla^2 v$$

$$w_t + uw_x + vw_y + ww_z = -p_z + \frac{1}{R_n} \nabla^2 w$$

$$u_x + v_y + w_z = 0$$

The Navier-Stokes equations can be obtained by a transformation for computation.

$$u_t + U \cdot u_t + V \cdot u_\eta + W \cdot u_\zeta \\ = -(\xi_x P_\zeta + \eta_x P_\eta + \zeta_x P_\zeta) + 1/R_n \cdot \nabla^2 u$$

$$v_t + U \cdot v_t + V \cdot v_\eta + W \cdot v_\zeta \\ = -(\xi_y P_\zeta + \eta_y P_\eta + \zeta_y P_\zeta) + 1/R_n \cdot \nabla^2 v$$

$$w_t + U \cdot w_t + V \cdot w_\eta + W \cdot w_\zeta \\ = -(\xi_z P_\zeta + \eta_z P_\eta + \zeta_z P_\zeta) + 1/R_n \cdot \nabla^2 w$$

The continuity equation is obtained by transformation.

$$\xi_x u_t + \eta_x u_\eta + \zeta_x u_\zeta + \xi_y v_t + \eta_y v_\eta + \zeta_y v_\zeta + \xi_z w_t \\ + \eta_z w_\eta + \zeta_z w_\zeta = 0$$

where U, V, W are contravariant velocities.

$$U = \xi_x u + \xi_y v + \xi_z w$$

$$V = \eta_x u + \eta_y v + \eta_z w$$

$$W = \zeta_x u + \zeta_y v + \zeta_z w$$

The free surface is moved by the following equation.

$$\delta \zeta / \delta t + u \cdot \delta \zeta / \delta x + v \cdot \delta \zeta / \delta y - w = 0 |_{z=\zeta}$$

